Space Weather

RESEARCH ARTICLE
10.1029/2022SW003047

Key Points:

- A prediction method for short-term (1–24) h f_oF_2
- The method is efficient under low magnetic activity to distinguish negative and positive Q-disturbances
- The method is also efficient under magnetically disturbed conditions with shorter lead times

Correspondence to:

L. Perrone,
loredana.perrone@ingv.it

Citation:

Perrone, L., & Mikhailov, A. V. (2022). SRF2—A short-term (1–24)h f_oF_2 prediction method. *Space Weather*, *20*, e2022SW003047. https://doi.org/10.1029/2022SW003047

Received 27 JAN 2022
Accepted 19 JUN 2022

Author Contributions:

Conceptualization: L. Perrone, A. V. Mikhailov
Funding acquisition: L. Perrone
Investigation: L. Perrone, A. V. Mikhailov
Methodology: L. Perrone, A. V. Mikhailov
Software: L. Perrone, A. V. Mikhailov
Validation: L. Perrone, A. V. Mikhailov
Writing – original draft: L. Perrone, A. V. Mikhailov
Writing – review & editing: L. Perrone, A. V. Mikhailov

SRF2—A Short-Term (1–24)h f_oF_2 Prediction Method

L. Perrone[1] and A. V. Mikhailov[1,2]

[1]Istituto Nazionale di Geofisica e Vulcanologia (INGV), Via di Vigna Murata, Roma, Italia, [2]Pushkov Institute of Terrestrial Magnetism, Ionosphere and Radio Wave Propagation (IZMIRAN), Moscow, Russia

Abstract A sunrise F_2-layer short-term (1–24) h f_oF_2 prediction method has been developed to forecast f_oF_2 variations at a given ionosonde station during magnetically quiet and disturbed periods. The proposed method efficiently describes both positive and negative quiet time F_2-layer disturbances under daily Ap <30 nT and this was done for the first time. A comparison with modern global empirical models demonstrates a statistically significant advantage over them under various seasons and levels of solar activity.

Plain Language Summary A new method to predict hourly f_oF_2 with a lead time of (1–24) h at an ionosonde station has been proposed. Input information to run the derived method includes: hourly real-time f_oF_2 observations, a monthly Australian T-index to specify the median f_oF_2 background level, and a predicted level of geomagnetic activity with two gradations: quiet (daily Ap < 30 nT) and disturbed (daily Ap ≥ 30 nT). The method is efficient to predict both negative and positive quiet time F_2-layer disturbances and this is done for the first time. The method is also efficient under magnetically disturbed conditions but with shorter lead times. The prediction accuracy is significantly better than global empirical IRI (STORM) and GDMF2 models provide. This is valid for any season and level of solar activity. All these open wide possibilities for the method's application in practice.

1. Introduction

Despite long history and many undertaken attempts, the problem of short-term (1–24) h f_oF_2 prediction has not been yet satisfactorily solved due to many objective reasons. This issue was discussed in detail in our previous paper (Mikhailov & Perrone, 2014), where a new prediction method has been proposed, which was implemented in the EUROMAP prediction model. However, the follow-on analysis has revealed serious limitations of that method, which may be formulated as follows.

1. Traditionally, variations of the F_2-layer parameters (f_oF_2 in particular) are related to global indices of solar ($F_{10.7}$) and geomagnetic (ap or Kp) activities (e.g., Araujo-Pradere et al., 2002; Araujo-Pradere & Fuller-Rowell, 2002; Shubin & Deminov, 2019), while the F_2-layer manifests strong spatial and temporal variations during both magnetically quiet and disturbed periods. Such variations mainly reflect the state of the surrounding thermosphere (neutral composition, temperature, and winds), and global indices are not very efficient to describe local variations of thermospheric parameters.
2. Along with storm-time f_oF_2 variations, there are quiet time F_2-layer disturbances (Q-disturbances) (Mikhailov et al., 2004), which occur under magnetically quiet conditions, and the magnitude of such f_oF_2 perturbations is comparable to F_2-layer storm effects. Our recent analyses (Mikhailov et al., 2021; Perrone et al., 2020) have shown that daytime Q-disturbances are due to atomic oxygen and thermospheric wind day-to-day variations, which are not properly described by empirical thermospheric models based on global solar and geomagnetic activity indices.

   Figure 1 gives some examples of f_oF_2 Q-disturbances observed at Boulder in a comparison with the monthly median and the IRI (STORM) (Araujo-Pradere et al., 2002) model predictions. Daytime f_oF_2 Q-disturbances may be very strong up to a factor of two (four times in N_mF_2) with respect to the monthly median level, and this is comparable to f_oF_2 deviations during severe magnetic storms. The IRI (STORM) model does not describe such disturbance cases as this is seen in Figure 1. The IRI (STORM) model is driven by an index based on the integral of the planetary 3-hourly a_p indices over the previous 33 hr, weighted by a special filter. For magnetically quiet periods ($D_{st} > -50$ nT), "the model does not normally predict any change from the monthly mean" (Araujo-Pradere & Fuller-Rowell, 2002); in other words, it does not predict the Q-disturbances. Therefore, the problem of Q-disturbances prediction is a very actual one from a practical point of view. However, this issue is not discussed in the literature devoted to ionospheric prediction.

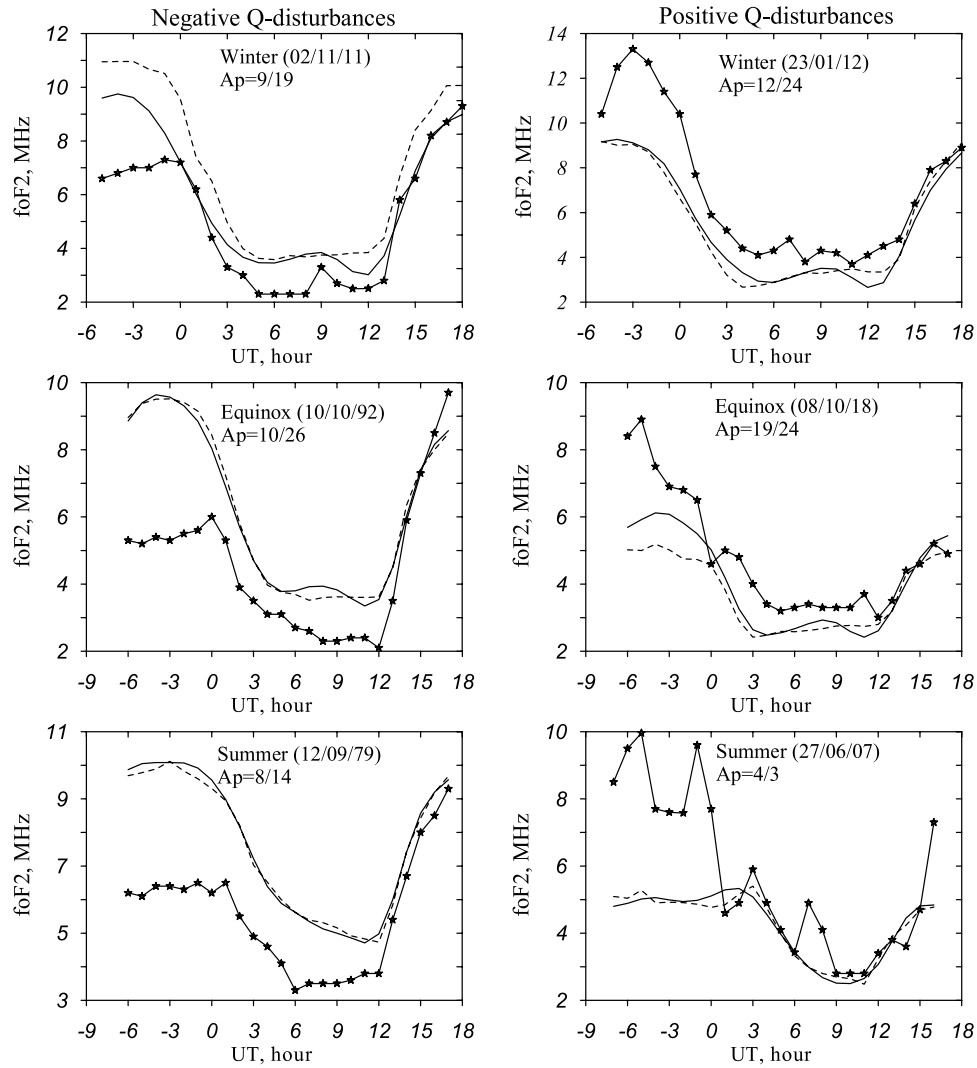

Figure 1. Some examples of negative and positive f_oF_2 Q-disturbances (asterisks) observed at Boulder in three seasons. IRI (STORM) model (solid line) and monthly median (dashes) f_oF_2 variations are given for a comparison. Daily Ap for the current and previous days is given in plots. Negative UT corresponds to previous days.

3. The EUROMAP model, also based on global ap(τ) indices (Wrenn, 1987), is unable to distinguish positive and negative f_oF_2 disturbances under low ap(τ) values. Figure 2 taken from (Mikhailov & Perrone, 2014) clearly demonstrates this drawback of the EUROMAP model. A cloud of points within ±30% for the f_oF_2/f_oF_{2bgr} (observed/background) ratio is seen for ap(τ) < 30. Bearing in mind that Q disturbances are numerous, such unpredictable scatter in f_oF_2 is absolutely unacceptable from a practical point of view.

Therefore, the aim of our paper is to propose a prediction method for the short-term (1–24) h f_oF_2 forecast bearing in mind the following aspects.

1. The method should be efficient under low magnetic activity to distinguish negative and positive Q-disturbances as in practice a priori the type (positive/negative) of future disturbance is not known.
2. The method should be also efficient under magnetically disturbed conditions, describing at least the negative storm phase in f_oF_2 variations, which is the most important from a practical point of view.
3. Keeping in mind practical applications, the method should be based on all available input information.
4. Comparative possibilities of the proposed method should be manifested using available global models and hourly f_oF_2 observations.

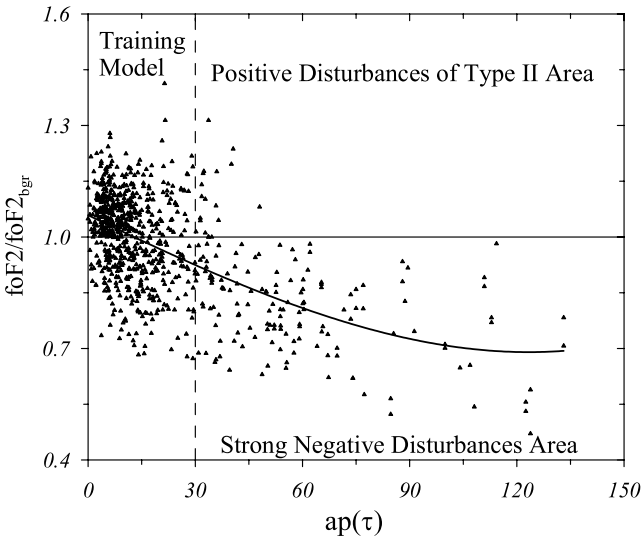

Figure 2. The f_oF_2/f_oF_{2bgr} ratio versus ap(τ) index (from Mikhailov & Perrone, 2014).

2. Method Description

Electron concentration N_mF_2 in the middle- and low-latitude F_2 regions mainly depends on the incident solar EUV flux, neutral composition, and vertical plasma drift related to the horizontal thermospheric winds at middle latitudes and zonal electric fields in the vicinity of the geomagnetic equator (Rishbeth & Garriott, 1969). Solar EUV is a slowly varying quantity and normally it may be considered as a constant for neighboring days in question. However, both neutral composition and vertical plasma drift manifest strong spatial and temporal variations even under quiet conditions and their variations are not satisfactorily described by modern empirical models. We do not mention first-principle models, which at present cannot compete with empirical ones (Bruinsma et al., 2018; Shim et al., 2011, 2012; Tsagouri et al., 2018). This issue was discussed by Schunk et al. (2012).

The only possibility as this is seen from now is using local (at each ionosonde station) observed f_oF_2 variations, which manifest the current state of the surrounding thermosphere. Keeping in mind that the characteristic time of thermospheric parameters' variations is long enough (7–12) h according to Hedin (1987), one may hope to get a satisfactory f_oF_2 prediction within this characteristic time.

According to the present-day understanding of the thermosphere-ionosphere interaction, auroral heating by magnetospheric electric fields and particle precipitation is the main process controlling day-to-day variations of the thermosphere (e.g., Perrone et al., 2020; Mikhailov et al., 2021). The intensity of this heating depends on the level of geomagnetic activity; however, it takes place under low magnetic activity as well and F_2-layer Q disturbances demonstrate this impact (Mikhailov et al., 2021; Perrone et al., 2020). Thermospheric circulation is equatorward during nighttime hours (Drob et al., 2015), transferring the perturbed neutral composition from the auroral zone to middle and lower latitudes. Therefore, the sunrise hours may serve as an indicator of fresh neutral composition (O/N_2 ratio) arrived at a given location during previous nighttime hours. The idea of using sunrise hours to specify the O/N_2 ratio was used by Rishbeth et al. (1995) to explain "seasonal sunrise anomaly." In both cases, the idea is the same—Larger df_oF_2/dt during sunrise hours corresponds to a larger O/N_2 ratio. In our case, considering day-to-day f_oF_2 variations, larger O/N_2 should correspond to positive f_oF_2 disturbances, while a lower sunrise O/N_2 ratio should result in negative f_oF_2 deviations with respect to monthly median values. Four f_oF_2 values observed after the local sunrise are used to specify df_oF_2/dt in our prediction method. Although the relationship between daytime f_oF_2 and the sunrise df_oF_2/dt does exist, our analysis has shown that it is not sufficient for an accurate f_oF_2 prediction. The problem is in vertical plasma drift related to thermospheric winds and electric fields, which strongly affects diurnal f_oF_2 variations. Therefore, along with the sunrise df_oF_2/dt, the currently observed hourly f_oF_2 is used in the prediction method. The forecast starts at the (UTsr + 4h) moment when df_oF_2/dt is specified, UTsr being the UT moment of the local sunrise at the ground level. This df_oF_2/dt is kept unchanged for 24 hr until the next sunrise, while the currently observed hourly f_oF_2 coming from each UT moment is used for a new f_oF_2 forecast with (1–24) h lead time, n. Therefore, the following regression is used in the prediction method.

$$\delta f_oF_2\,(UT + n) = c_0 + c_1\delta f_oF_2(UT) + c_2\,(df_oF_2/dt) \quad (1)$$

where $\delta f_oF_2 = f_oF_2/f_oF_{2med}$ and f_oF_{2med} is the monthly median (see later); c_i is the regression coefficients to be specified.

Normally, at least 25–30 years with hourly f_oF_2 observations (without large gaps) are required to create a prediction model at a given station. All months with f_oF_2 observations are divided into three groups in accordance with the level of solar activity (SA in $F_{10.7}$ units) using the 12-month running mean $F_{10.7}$ as an index: solar minimum $SA < 85$, solar medium $85 \le SA \le 150$, and solar maximum $SA > 150$. A division of data in accordance with solar activity level is necessary as diurnal variations of median foF_2 and storm effects depend on the solar activity level. Only two gradations: quiet—daily $Ap < 30$ nT and disturbed—daily $Ap \ge 30$ nT are used to divide data in the magnetic activity. Three consecutive days are analyzed for the Ap index as we work with UT time and

depending on the longitude of a station, different days are used. Quiet conditions: previous, current, and next day should have Ap < 30 nT. Disturbed conditions: either all 3 days have Ap ≥ 30 nT, or previous and current days have Ap ≥ 30 nT, or only one previous day should be with Ap ≥ 30 nT.

Regression coefficients in (1) for quiet conditions can be found for all 12 months of the year as the number of quiet time days is sufficient for this. However, the number of really disturbed days is limited and all observed cases were grouped into three seasons: winter, equinox, and summer with corresponding regression coefficients. The coefficients are calculated for 24 UT moments of the forecast issuing with (1–24) lead times. Therefore, each set of coefficients for a month/season includes $24 \times 24 \times 3 = 1728$ coefficients and the total number for 12 months and 3 levels of solar activity equals 62208 coefficients for Q-disturbances and 15552 for D-disturbances as only 3 seasons are considered.

A selection of the monthly median (the background level) is a crucial point for any prediction method. This issue was discussed in our previous paper (Mikhailov & Perrone, 2014); therefore, we do not repeat it here. We have derived local (for each station) monthly median f_oF_2 models, which are based on the ionospheric T-index (Caruana, 1990; Turner, 1968) as an indicator of solar activity. It is well-known that effective ionospheric indices of solar activity provide the best correlation with the monthly median f_oF_2 (e.g., Mikhailov & Mikhailov, 1999). Such local models may be used as the background to calculate f_oF_2 deviations. It is assumed that the median is appropriate for the sixteenth day of a month. Using f_oF_2 medians for neighboring months, it is possible to create a "median" for each day of a month and each UT moment (Wrenn et al., 1987). However, such medians may be considered as "climate" but we need "weather." The following analysis has shown that "weather" may be provided by adding to the "climate" median a 13-day running median calculated over 13 previous days using the observed f_oF_2. It was found that a half sum of model and 13-day running medians provided the best results and namely such medians are used in the prediction method.

3. Results

To illustrate the possibilities of the proposed method, local prediction models were derived for five midlatitude stations located in different longitudinal sectors: Moscow (55.5°N and 37.3°E), Tunguska (61.6°N and 90.0°E), Magadan (60.1°N and 151.0°E), Boulder (40.0°N and 254.7°E), Slough/Chilton (51.5°N and 359.4°E), one equatorial station, Huancayo (12.0°S and 284.7°E) located at the geomagnetic equator, and Sodankylä (67.4°N and 26.6°E) located in the auroral zone. Of course, the preference should be given to old manually developed f_oF_2 observations and in fact their amount is sufficient to analyze that quiet time conditions but all available observations, including recent automatically scaled f_oF_2 data, were used for disturbed events, as the number of such cases is limited.

3.1. Midlatitude Stations

The most interesting and important from a practical point of view result is a capability of the method to describe Q disturbances; distinguishing negative from positive ones, this feature was absent in our previous EUROMAP model. Some examples are given in Figure 3 for Moscow in a comparison with the IRI (STORM) model and the running median. The forecasts with lead time n = (1–24) h given in plots were issued at the (UTsr +4h) moment where UTsr—Integer UT close to the local sunrise.

The examples given in Figure 3 tell us that good prediction results with the lead time of up to 24 hr can be obtained for Q disturbances with the proposed method and this result has been achieved for the first time.

Now let us consider statistical results obtained over all available f_oF_2 observations at five midlatitude ionosonde stations in question. The predicted with lead time n = (1–24) h mean relative deviations MRD = $\sum(f_oF_{2mod}/f_oF_{2obs})/N$ (in %), route mean square RMS = $(\sum(f_oF_{2obs} - f_oF_{2mod})^2/N)^{1/2}$ (in MHz), and Bias = $\sum(f_oF_{2obs} - f_oF_{2mod}/)/N$ (in MHz) were compared with the running median and two empirical models, IRI (STORM) by Araujo-Pradere et al. (2002) and GDMF2 by Shubin and Deminov (2019). Testing the method, we tried to be as much as possible close to the real situation when we have a prediction model derived for a particular ionosonde station, hourly f_oF_2 observations, and a qualitative prediction (quiet/disturbed) of geomagnetic activity. Quantitatively, this threshold corresponds to Ap ~30 nT. Daily Ap indices are now routinely predicted (1–3) days in advance and may be found at the Prediction center sites: http://www.nwra.com/spawx/list27do.html; http://www.ips.gov.au/Geophysical/3/1;

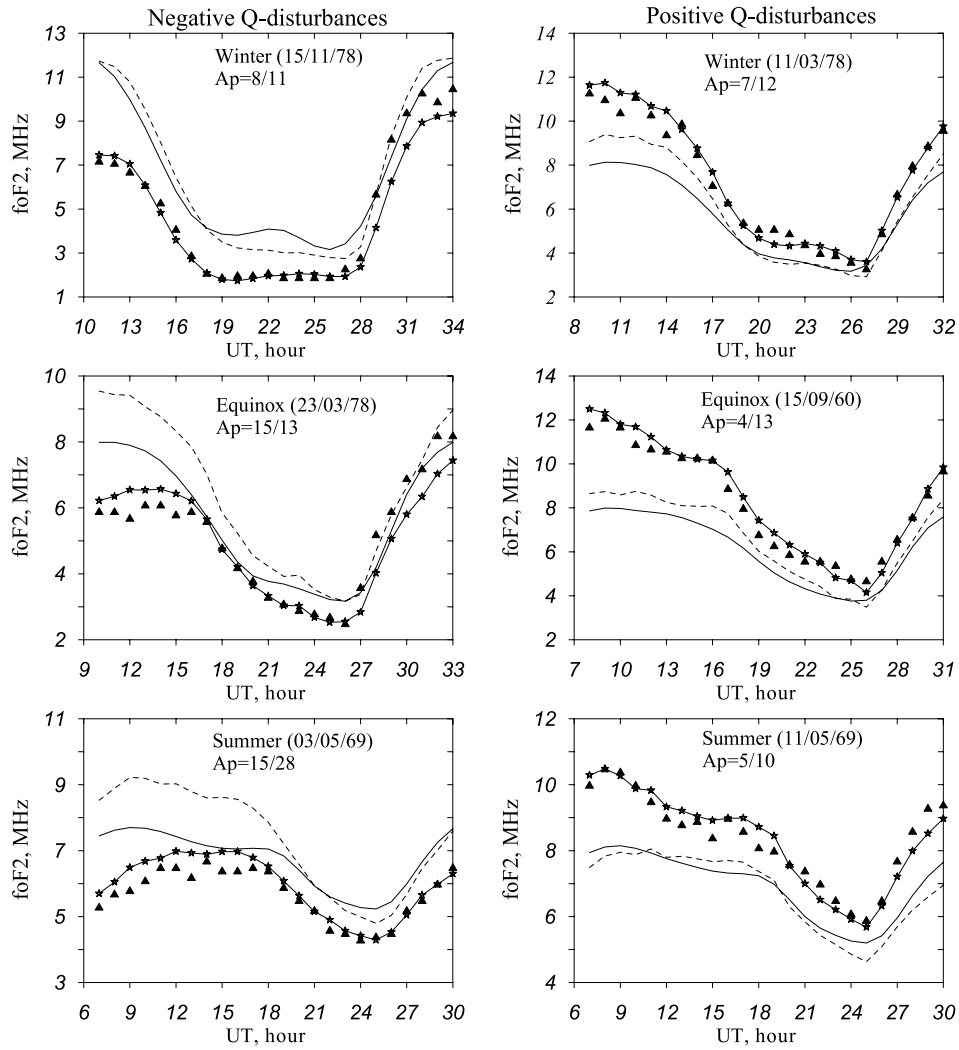

Figure 3. Examples of Q disturbances predicted with the new method. Observed at Moscow f_oF_2 (triangles) are given along with the predicted (asterisks), IRI (STORM) (solid line), and running median (dashes) variations. Each forecast given in plots was issued at the (UTsr +4h) moment, UTsr—integer UT close to the local sunrise.

http://sidc.oma.be/products/meu/. Local (at each station) monthly median f_oF_2 models are fed with Australian ionospheric indices T (https://www.sws.bom.gov.au/HF_Systems/6/4/1), which are available with a large lead time. Season/month and the phase of solar activity (minimum, middle, or high) are always known. This is the list of input parameters necessary to issue the f_oF_2 forecast with a (1–24) h lead time at a given station.

In accordance with the earlier mentioned rules, all dates were divided into two groups—Quiet and disturbed. In each group, only days with $\delta = f_oF_2/f_oF_{2med} \geq 1.25$ (positive disturbances) and ≤ 0.75 (negative disturbances) during 3 consecutive daytime hours were selected for testing. The selected days in this way were further divided into three seasons (winter, equinox, and summer). The IRI (STORM) and GDMF2 models were used for a comparison—Both empirical models are included in the IRI model. During this testing, both empirical models turned out to be in "soft" conditions, which means that really observed magnetic indices were used as input information. In real situation, only predicted magnetic indices are available for these empirical models, but the accuracy of such predictions is not very high (e.g., Mikhailov & Perrone, 2014).

Figures 4 and 5 (for Moscow and Boulder as an example) give mean relative deviations MRD (not to overload the plots with other metrics) versus lead time for the newly proposed method in a comparison with two empirical models and the running median. Of course, the term "lead time" has sense only for the prediction method; for the empirical models, it just specifies the UT moment to take observed magnetic indices as input information. Results

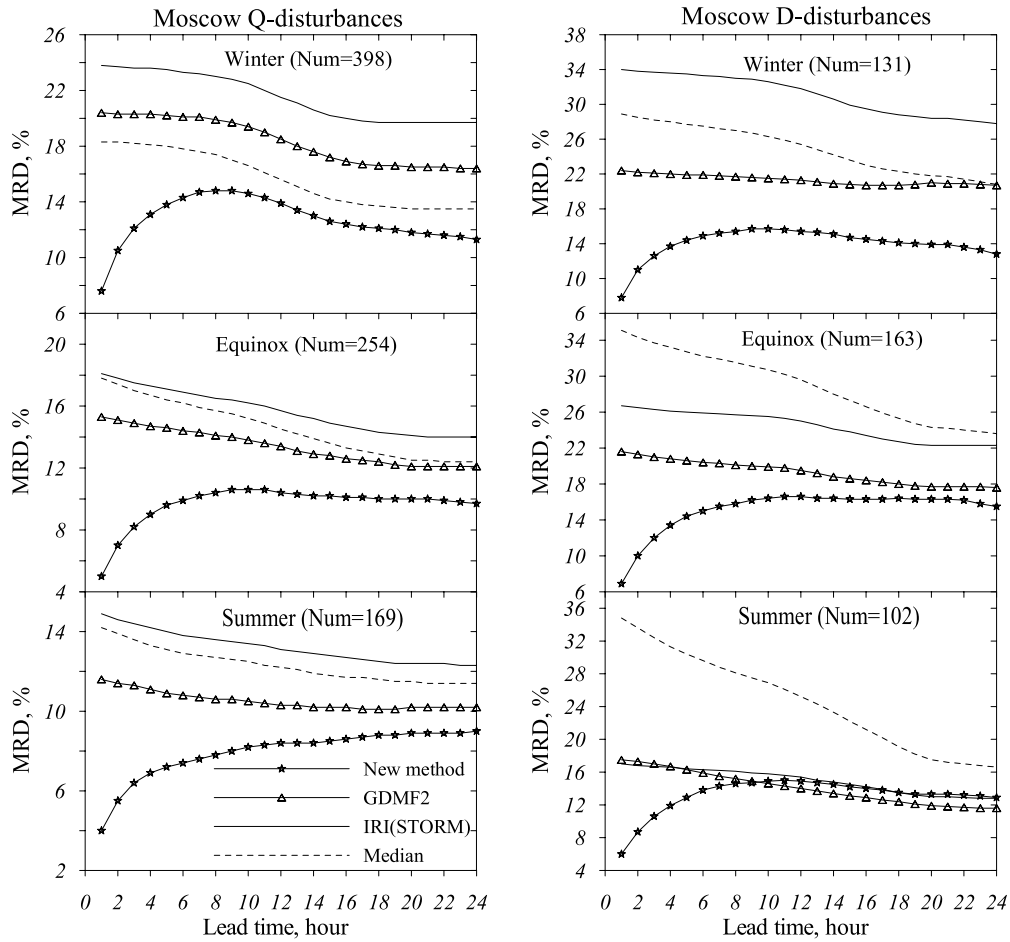

Figure 4. Mean relative deviations (MRD in %) versus lead time at Moscow. Predicted MRD using the newly proposed method is compared with two empirical models and the running median. Left column—Results for Q disturbances, right column—For D disturbances. The number of analyzed days is given at the top of plots.

for Q-disturbance cases (Figures 4 and 5 similar for other stations) show that the proposed method provides the best description accuracy in the majority of cases for three seasons.

The difference with other models and the running median for Q disturbances is statistically significant (the level >95%) according to the Student t-criterion. The only exclusion manifests Boulder in the summer period for lead times >14 hr when running median provides the same accuracy (Figure 5 left-bottom panel).

Results for magnetically disturbed days (right columns in Figures 4 and 5) are different. First, MRD is systematically larger for disturbed periods compared to quiet ones. This takes place both for predicted and model values, although the general pattern is mainly the same for the two selections of dates. The proposed method systematically provides the best results for small lead times <7 hr. The largest advantage over other models and the running median takes place in winter for all lead times. However, in summer, the advantage over the IRI (STORM) model takes place only for the first ~7 hr. The equinoctial period demonstrates intermediate results and depending on the station, the advantage of the new method over other empirical models may take place for the first 10–12 hr. In any case, the obtained results may be considered as interesting and important from a practical point of view.

Similar analysis was done for five midlatitude ionosonde stations using all available hourly f_oF_2 observations, and the results for Q- and D-disturbance cases are given in Table 1 for three seasons. Mean over five stations MRD (in %), RMS (in MHz), and Bias (in MHz) are given in Table 1. The total number of analyzed days in each case is given in the headline of the table. The results are presented only for five lead times (1, 3, 6, 12, and 24) h not to overload the table.

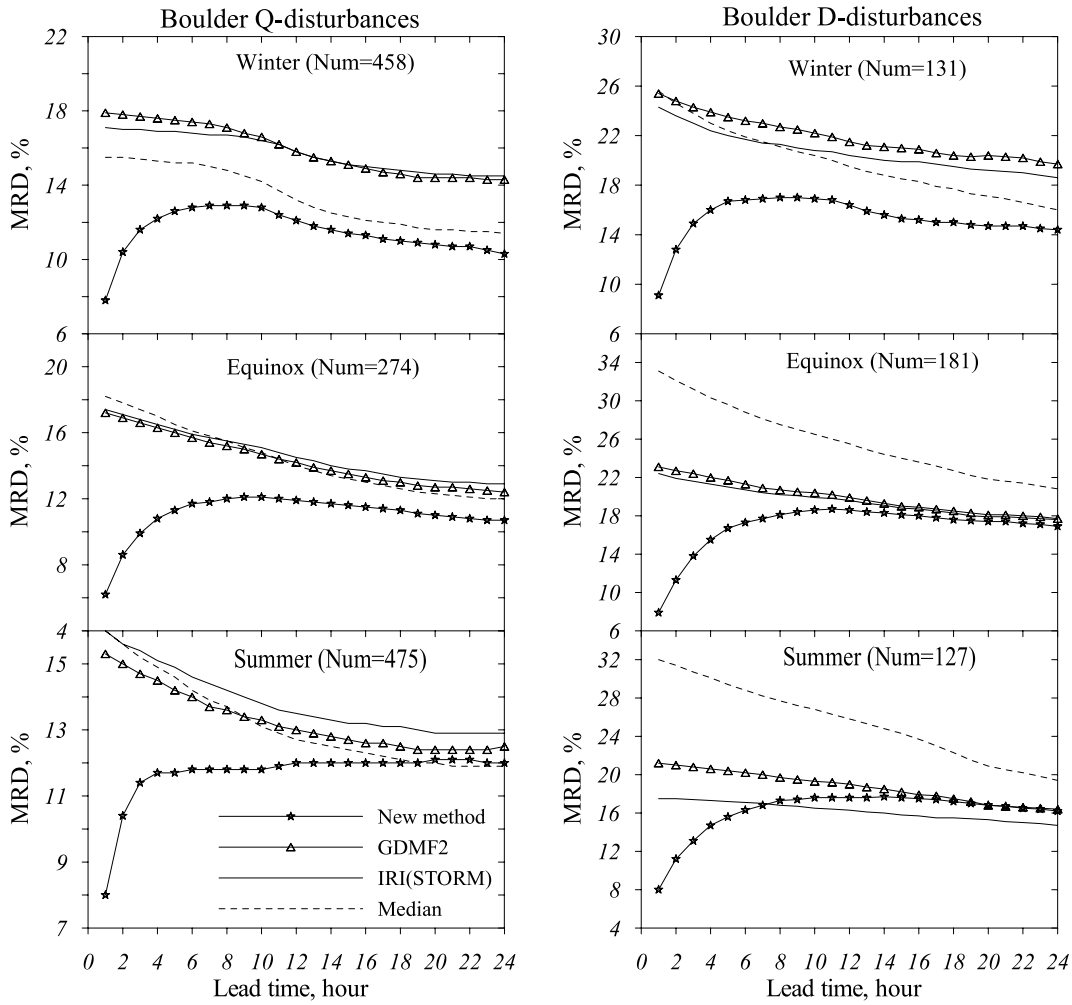

Figure 5. Same as Figure 4 but for Boulder.

Mean over five stations results clearly manifest that the proposed SRF2 method provides the best results for the majority of analyzed cases both for Q- and D-disturbance dates. Due to the large number of cases, the difference between IRI (STORM) and GDMF2 models is statistically significant according to the Student t-criterion. The only exception manifests D-disturbance cases in summer under large lead times when GDMF2 provides statistically significant the best results.

Table 1 gives the descriptive accuracy of the SRF2 method as same years were used both for the model derivation and testing, while normally different sets of observations should be used for an accurate model testing. Unfortunately, this not always can be done bearing in mind limited amount of available observations, especially for disturbed cases related to magnetic storms. Such a division of periods was possible for stations like Slough/Chilton and Moscow with long enough series of observations and only to test Q disturbances, which are much more numerous compared to D disturbances related to magnetic storms. At Moscow, 30 years were used to derive model coefficients and 15 years—For testing Q disturbances. At Slough/Chilton—33 and 19 years, correspondingly. Mean of the two stations MRD (in %), RMS (in MHz), and Bias (in MHz) calculated over 2-year selections (for a comparison) are given in Table 2, which is arranged similar to Table 1.

The results of Table 2 confirm the earlier obtained conclusion—The SRF2 method manifests statistically better results compared to GDMF2, IRI (STORM), and local medians for 2-year selections—One for years used to drive the model coefficients and the other for years not used for the model derivation. This result is of practical importance bearing in mind the application of the SRF_2 method. On the other hand, a comparison of the 2-year selections has shown that the difference according to t-criterion is insignificant for the equinox and winter

Table 1
Mean Relative Deviations (MRD (in %), RMS (in MHz), and Bias (in MHz) Over 5 Stations for Q and D Disturbances During Three Seasons for Some Lead Times, n

Winter, Q disturbances (Num = 1869)						Winter, D disturbances (Num = 519)			
n, hour	Metric	SRF_2	$GDMF_2$	IRI_{STORM}	Median	SRF_2	$GDMF_2$	IRI_{STORM}	Median
1	MRD	**7.8**	18.1	22.8	17.5	**9.0**	20.7	29.9	27.4
	RMS	**0.53**	1.11	1.25	−0.11	**0.60**	1.26	1.42	1.50
	Bias	**0.00**	−0.29	−0.06	1.01	**−0.01**	−0.23	0.45	0.56
3	MRD	**12.2**	19.6	22.7	17.4	**15.0**	21.8	29.0	26.2
	RMS	**0.74**	1.20	1.24	0.99	**0.94**	1.32	1.35	1.38
	Bias	**−0.01**	−0.29	−0.06	−0.10	**−0.01**	−0.28	0.39	0.49
6	MRD	**14.1**	20.1	22.5	17.0	**17.3**	22.2	28.3	24.7
	RMS	**0.81**	1.23	1.22	0.96	**1.07**	1.36	1.32	1.27
	Bias	**−0.02**	−0.30	−0.06	−0.10	**0.03**	0.32	0.35	0.42
12	MRD	**13.6**	19.5	21.3	15.1	**16.7**	22.1	27.1	22.2
	RMS	**0.79**	1.24	1.18	0.89	**1.05**	1.38	1.29	1.17
	Bias	**0.01**	−0.27	−0.03	−0.07	**0.06**	0.31	0.34	0.37
24	MRD	**11.4**	17.2	20.3	13.3	**14.4**	19.5	24.8	18.5
	RMS	**0.69**	1.07	1.15	0.84	**0.94**	1.22	1.23	1.06
	Bias	0.02	−0.21	**−0.01**	−0.04	**0.00**	−0.23	0.32	0.31
Equinox, Q disturbances (Num = 1125)						Equinox, D disturbances (Numr = 659)			
n, hour	Metric	SRF_2	$GDMF_2$	IRI_{STORM}	Median	SRF_2	$GDMF_2$	IRI_{STORM}	Median
1	MRD	**5.6**	14.7	19.6	18.6	**7.7**	21.4	28.1	36.1
	RMS	**0.43**	1.10	1.36	1.34	**0.50**	1.21	1.40	1.86
	Bias	**0.00**	−0.24	−0.14	−0.14	**−0.01**	0.26	0.61	1.24
3	MRD	**9.0**	15.3	19.1	17.8	**13.5**	20.8	27.3	34.4
	RMS	**0.67**	1.15	1.31	1.28	**0.83**	1.17	1.36	1.76
	Bias	**0.01**	−0.25	−0.15	−0.15	**0.02**	0.21	0.56	1.15
6	MRD	**10.8**	15.3	18.4	16.8	**16.7**	19.8	26.4	32.2
	RMS	**0.80**	1.16	1.25	1.19	**1.03**	1.11	1.31	1.63
	Bias	**0.01**	−0.28	−0.17	−0.18	**0.08**	0.14	0.50	1.04
12	MRD	**11.4**	15.0	17.3	15.1	**17.4**	18.6	25.0	28.2
	RMS	**0.85**	1.14	1.19	1.10	**1.08**	1.07	1.27	1.45
	Bias	**0.00**	−0.30	−0.19	−0.20	**0.10**	0.03	0.43	0.85
24	MRD	**10.8**	13.9	15.8	13.3	**16.4**	17.1	22.7	22.5
	RMS	**0.83**	1.09	1.14	1.03	**1.10**	1.06	1.24	1.32
	Bias	**−0.03**	−0.30	−0.21	−0.21	**0.06**	−0.01	0.36	0.65
Summer, Q disturbances (Num = 1006)						Summer, D disturbances (Num = 450)			
n, hour	Metric	SRF_2	$GDMF_2$	IRI_{STORM}	Median	SRF_2	$GDMF_2$	IRI_{STORM}	Median
1	MRD	**5.1**	11.9	15.9	15.3	**6.5**	14.8	17.1	32.3
	RMS	**0.46**	0.97	1.28	1.20	**0.44**	0.86	1.01	1.63
	Bias	**0.01**	−0.36	−0.60	−0.44	**−0.01**	0.19	0.15	1.20
3	MRD	**7.9**	12.2	15.4	14.6	**11.2**	15.7	16.8	30.7
	RMS	**0.65**	0.99	1.23	1.14	**0.72**	0.93	1.00	1.57
	Bias	**0.01**	−0.33	−0.57	−0.40	**0.01**	0.16	0.12	1.11

Table 1
Continued

Summer, Q disturbances (Num = 1006)						Summer, D disturbances (Num = 450)			
n, hour	Metric	SRF_2	$GDMF_2$	IRI_{STORM}	Median	SRF_2	$GDMF_2$	IRI_{STORM}	Median
6	MRD	**9.2**	12.3	14.7	13.8	**14.2**	16.0	16.5	28.6
	RMS	**0.73**	0.98	1.18	1.08	**0.88**	0.97	0.99	1.49
	Bias	**0.01**	−0.29	−0.52	−0.36	**0.04**	0.11	0.08	0.99
12	MRD	**10.0**	11.9	13.9	12.7	**15.3**	15.5	15.6	25.2
	RMS	**0.78**	0.95	1.11	1.00	**0.95**	0.96	0.95	1.35
	Bias	**0.01**	−0.25	−0.47	−0.31	**0.05**	0.01	0.06	0.80
24	MRD	**10.0**	11.2	13.0	11.5	**13.8**	13.7	14.0	18.0
	RMS	**0.79**	0.91	1.05	0.93	**0.95**	0.93	0.93	1.11
	Bias	**0.00**	−0.22	−0.42	−0.25	**0.01**	−0.08	−0.02	0.50

Note. The new SRF2 method is compared to the running median and two empirical models. The best results are given in bold. The total number of analyzed days is given in the headlines.

seasons and is significant in summer. No explanation to this seasonal difference can now be suggested. Tables 1 and 2 also indicate that the bias is very small, telling us that the method is well-centered with respect to observations. This is not surprising. Ionospheric foF_2 observations are obtained with one and the same method (vertical sounding), and the method of ionogram scaling is also the same regulated by the U.R.S.I. Handbook of Ionogram Interpretation and Reduction (Piggott & Rawer, 1978). Therefore, foF_2 observations are homogeneous in two groups of data—Used to derive model coefficients and those used for testing. Model regression coefficients are obtained with the least squares method, which guarantees that the model is centered.

3.2. Equatorial and Auroral Stations

The formation mechanism of the equatorial and auroral F_2 layers is different from the midlatitude one; therefore, a special analysis was required to estimate the efficiency of the proposed method in such conditions. Vertical ExB plasma drift is the main factor responsible for the variability of f_oF_2 in the vicinity of the geomagnetic equator. Zonal electric field E is produced via the dynamo-mechanism (Rishbeth & Garriott, 1969), which depends on the thermospheric circulation at E-region heights. Penetrating high-latitude electric fields (Kamide & Matsushita, 1981) also contribute to the variability of the zonal electric field at the geomagnetic equator, especially during magnetically disturbed periods. The role of neutral composition in the f_oF_2 variability is less compared to that related to ExB plasma drifts. Therefore, it is interesting to check whether the proposed method is able to catch the specificity of the equatorial f_oF_2 variations. The basic version of the SRF2 method was used in this testing. The results are given in Figure 6 for Q- and D-disturbance cases during three seasons (summer/winter months are inversed in the Southern Hemisphere). The small number of available disturbed cases is a specific feature of this equatorial station.

By analogy with midlatitude stations, the proposed method manifests the best results both for Q and D conditions, but unlike middle latitudes, the running median demonstrates better results for large lead times compared to the global empirical models.

The difference between the new method and the running median is significant (at the confidence level >95%) during the first (5–12) h for Q-disturbance cases. The difference is significant during 4 hr (in summer/winter) and 15 hr in equinox for D-disturbance cases. Vertical lines in Figure 6 indicate the 95% significance level. Bearing in mind the large variability of equatorial ExB drifts (Fejer & Scherliess, 2001), such results may be considered acceptable from a practical point of view.

The situation is much more complicated with the auroral zone. We have used Sodankylä observation to test the method. This is a good station with manually ionogram scaling and observations are available since 1958. However, large gaps in f_oF_2 observations are systematically present due to insufficient or a complete absence of direct solar ionization in winter. Auroral Es produced by particle precipitation often completely blankets f_oF_2

Table 2
Mean Relative Deviations (MRD) (in %), RMS (in MHz), and Bias (in MHz) Over Moscow and Slough/Chilton Stations for Q Disturbances During Three Seasons for Some Lead Times, n.

Winter, years used for the model (Num = 777)						Winter, years used for testing (Num = 377)			
n, hour	Metric	SRF_2	$GDMF_2$	IRI_{STORM}	Median	SRF_2	$GDMF_2$	IRI_{STORM}	Median
1	MRD	**7.6**	14.3	21.8	18.1	**8.3**	18.9	19.8	17.0
	RMS	**0.52**	0.88	1.26	1.02	**0.50**	0.93	1.02	0.86
	Bias	**0.00**	−0.16	−0.14	−0.11	**0.00**	−0.08	−0.28	−0.16
3	MRD	**12.1**	18.2	21.6	18.0	**12.2**	18.8	19.6	16.9
	RMS	**0.72**	1.13	1.25	1.00	**0.65**	0.93	1.01	0.83
	Bias	**−0.01**	−0.18	−0.14	−0.11	**−0.01**	−0.07	−0.27	−0.14
6	MRD	**14.3**	19.6	21.3	17.6	**14.1**	18.7	19.5	16.7
	RMS	**0.80**	1.23	1.23	0.98	**0.69–**	0.92	1.01	0.81
	Bias	**−0.02**	−0.21	−0.15	−0.11	**0.05**	−0.06	−0.27	−0.14
12	MRD	**13.9**	20.0	19.6	15.5	**13.8**	17.2	17.9	14.6
	RMS	**0.79**	1.33	1.17	0.91	**0.69**	0.88	0.97	0.75
	Bias	**0.00**	−0.20	−0.13	−0.09	−0.05	**−0.04**	−0.25	−0.12
24	MRD	**11.2**	15.5	17.7	13.2	**11.0**	15.6	16.2	12.5
	RMS	**0.71**	0.96	1.13	0.86	**0.59**	0.83	0.92	0.68
	Bias	**0.00**	−0.12	−0.12	−0.07	**0.00**	0.00	−0.22	−0.09
Equinox, years used for the model (Num = 467)						Equinox, years used for testing (Num = 354)			
n, hour	Metric	SRF_2	$GDMF_2$	IRI_{STORM}	Median	SRF_2	$GDMF_2$	IRI_{STORM}	Median
1	MRD	**5.3**	10.9	18.2	18.4	**5.8**	11.1	18.5	18.1
	RMS	**0.41**	0.82	1.35	1.35	**0.44**	0.76	1.32	1.27
	Bias	**0.00**	−0.10	−0.26	−0.15	**0.00**	0.00	−0.31	−0.16
3	MRD	**8.5**	12.9	17.5	17.6	**9.1**	13.0	18.0	17.4
	RMS	**0.64**	0.98	1.30	1.28	**0.66**	0.92	1.28	1.21
	Bias	**0.00**	−0.11	−0.28	−0.17	**0.00**	−0.01	−0.17	−0.17
6	MRD	**10.1**	13.8	16.8	16.7	**10.9**	14.0	17.5	16.7
	RMS	**0.76**	1.07	1.24	1.19	**0.78**	1.01	1.24	1.14
	Bias	**−0.01**	−0.15	−0.31	−0.20	**0.00**	−0.02	−0.33	−0.19
12	MRD	**10.6**	14.3	15.6	14.9	**11.4**	14.4	16.1	14.9
	RMS	**0.82**	1.11	1.17	1.10	**0.84**	1.06	1.18	1.05
	Bias	**−0.01**	−0.17	−0.33	−0.22	**0.00**	−0.04	−0.34	−0.20
24	MRD	**10.0**	12.8	13.8	12.7	**10.4**	12.6	14.5	12.8
	RMS	**0.81**	1.01	1.11	1.02	**0.80**	0.96	1.13	0.99
	Bias	**−0.03**	−0.17	−0.34	−0.21	**−0.02**	−0.05	−0.35	−0.20
Summer, years used for the model (Num = 295)						Summer, years used for testing (Num = 100)			
n, hour	Metric	SRF_2	$GDMF_2$	IRI_{STORM}	Median	SRF_2	$GDMF_2$	IRI_{STORM}	Median
1	MRD	**4.6**	8.3	15.0	14.2	**6.0**	12.0	15.2	15.5
	RMS	**0.42**	0.73	1.26	1.17	**0.54**	0.93	1.14	1.09
	Bias	**0.01**	−0.22	−0.74	−0.52	**0.00**	−0.14	−0.43	−0.10
3	MRD	**7.2**	9.8	14.5	13.6	**9.4**	11.6	14.6	14.8
	RMS	**0.62**	0.85	1.22	1.12	**0.74**	0.88	1.09	1.02
	Bias	**0.01**	−0.19	−0.70	−0.48	**0.05**	−0.10	−0.38	−0.06

Table 2
Continued

Summer, years used for the model (Num = 295)						Summer, years used for testing (Num = 100)			
n, hour	Metric	SRF_2	$GDMF_2$	IRI_{STORM}	Median	SRF_2	$GDMF_2$	IRI_{STORM}	Median
6	MRD	**8.4**	10.6	14.0	13.0	**11.2**	11.3	14.1	14.1
	RMS	**0.70**	0.90	1.18	1.07	**0.81**	0.84	1.03	0.97
	Bias	**0.01**	−0.16	−0.66	−0.44	0.13	−0.06	−0.34	**−0.03**
12	MRD	**9.4**	11.0	13.1	12.1	12.0	**10.7**	13.3	13.0
	RMS	**0.77**	0.93	1.12	1.01	**0.82**	0.77	0.96	0.88
	Bias	**0.00**	−0.11	−0.60	−0.38	**0.15**	−0.03	−0.31	**0.00**
24	MRD	**9.4**	10.4	12.1	11.0	11.1	**10.1**	12.4	11.3
	RMS	**0.78**	0.89	1.05	0.94	0.81	**0.75**	0.92	0.82
	Bias	**−0.01**	−0.08	−0.53	−0.30	0.08	−0.04	−0.31	**−0.02**

Note. Left part of the table gives the results for years used to derive the model; right part—Independent validation. The best results are given in bold. The total number of analyzed days is given in the headlines.

observations especially during disturbed periods. For these reasons, the proposed method cannot be directly used in the auroral zone. Our analysis of monthly medians has shown that f_oF_2 diurnal variations always exhibit a minimum during morning hours, which systematically shift with UT in seasons. By analogy with the basic SRF2 method, this UT moment was considered as an "effective sunrise" UTsr and the f_oF_2 forecast was started after 4 hours, that is, at (UTsr + 4) moment. It should be noted that gaps in f_oF_2 observations are preliminary filled using the normalized local median and spline interpolation when this is necessary. However, due to a lack of available f_oF_2 observations, it was impossible to derive a prediction model for disturbed conditions.

Therefore, only comparison results for Q disturbances are given in Figure 7. The proposed method is seen to provide the best results for (1–24) h lead times in the summer and equinox, and only for the first 4 hr in winter compared to GDMF2. It is interesting to note that GDMF2 systematically manifests better results compared to IRI (STORM). Everywhere, the difference is statistically significant according to the Student t-criterion.

4. Discussion

For the first time, a method has been proposed to predict F_2-layer Q disturbances (both negative and positive) with an accuracy, which is statistically better (the confidence level >95%) than existing global empirical models provide. The result is valid for (1–24) h lead times, any season, and level of solar activity for the stations located equatorward of the auroral zone. At Sodankylä (the auroral zone), this takes place only in summer; for other seasons, the new method is more efficient only for the first (4–6) h lead times. The obtained result may be considered as interesting and important for practice as up to now we have not had any method to predict F_2-layer Q disturbances with an acceptable accuracy. Similar results are obtained when the proposed method demonstrates for disturbed periods when daily Ap ≥30 nT at all stations in question, excluding the auroral zone, where an insufficient amount of f_oF_2 observations during disturbed periods does not allow us to derive a prediction model. Using the GDMF2 model may be suggested as a possible solution during disturbed periods. This model unlike IRI (STORM) includes such specific features of the subauroral and auroral zones as the main ionospheric trough and the auroral oval.

The proposed method is very simple and is based on using hourly real-time f_oF_2 observations—In fact, this is the only crucial input information to provide the f_oF_2 forecast. Other input information, such as level of solar activity (low, middle, or high), monthly ionospheric T-index, and level of geomagnetic activity (quiet/disturbed—The threshold ~ 30 nT), is always available. From a practical point of view, this result may be considered as an important step toward the development of local (at particular ionosonde stations) f_oF_2 prediction models. In regions with a sufficient number of modern ionosondes (e.g., Europe), the proposed method may be successfully used for f_oF_2 short-term (1–24) h prediction under various geophysical conditions.

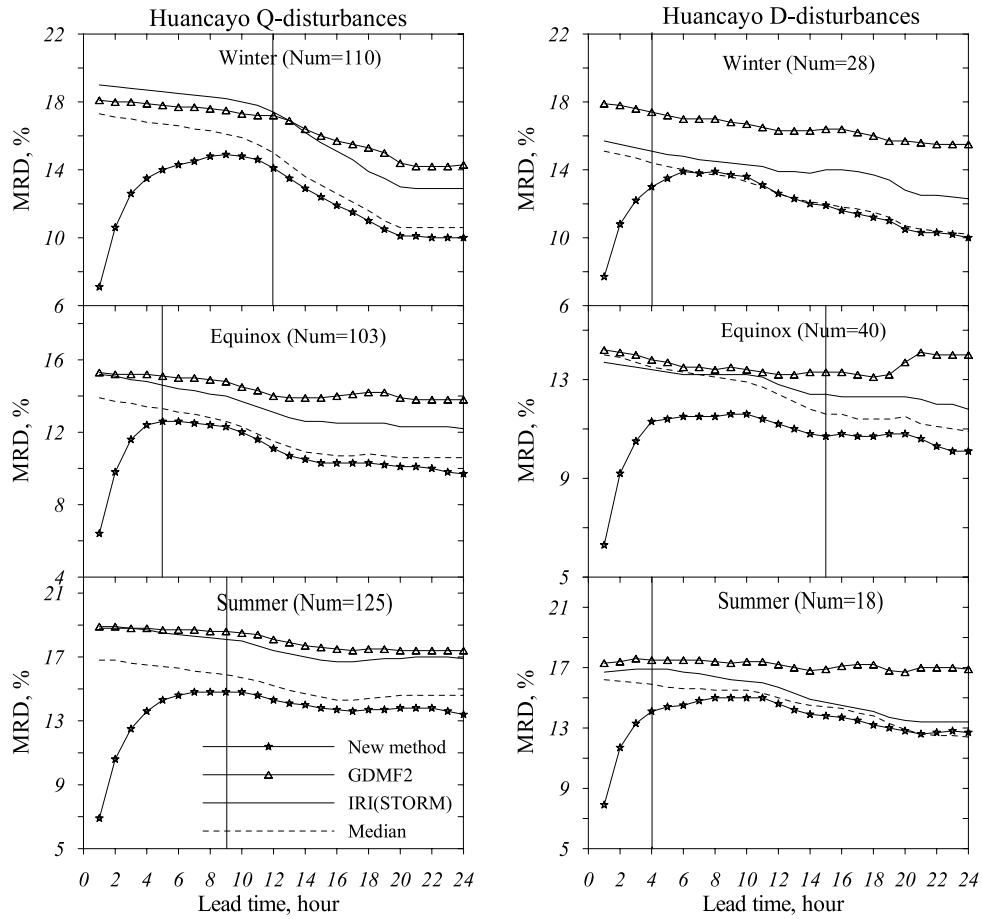

Figure 6. Same as Figure 4 but for Huancayo. Vertical lines indicate the 95% significance level for the difference with the running median.

Of course, the SRF2 method has some limitations. The method uses real-time f_oF_2 observations; therefore, a forecast made from nighttime (early morning) magnetically quiet period to future daytime magnetically disturbed hours may not be successful especially in summer during severe magnetic storms. Figure 8 gives some examples of such events at Juliusruh. Our forecasts were made at the (UTsr + 4) moment before the daytime onset of severe magnetic storms.

The method cannot describe the F_2-layer positive storm phase of type II occurring during daytime hours and the following negative storm phase (Figure 8) if a magnetic storm has started during daytime.

There are two types of positive F_2-layer disturbances (Mikhailov et al., 2012). Type I is characterized by prolonged (for many hours) positive foF_2 deviations of moderate magnitude, which are not followed by a negative F_2-layer storm phase. The effect is due to an increase in atomic oxygen abundance (Perrone et al., 2020). Such type of F_2-layer disturbances belongs to Q disturbances, and they may be efficiently described with our method. Type II—A short (2–4)h and strong foF_2 daytime increase related to an upsurge of the equatorward thermospheric wind during the initial phase of a magnetic storm. This is the first phase of a two-phase (positive/negative) F_2-layer storm, which is always followed by a negative storm phase related to the disturbed (low O/N_2) neutral composition arrived at middle latitudes from the auroral zone.

Figure 8 gives good examples of strong daytime magnetic storms with both (positive/negative) storm phases seen at middle latitudes. However, such severe magnetic storms are very rare.

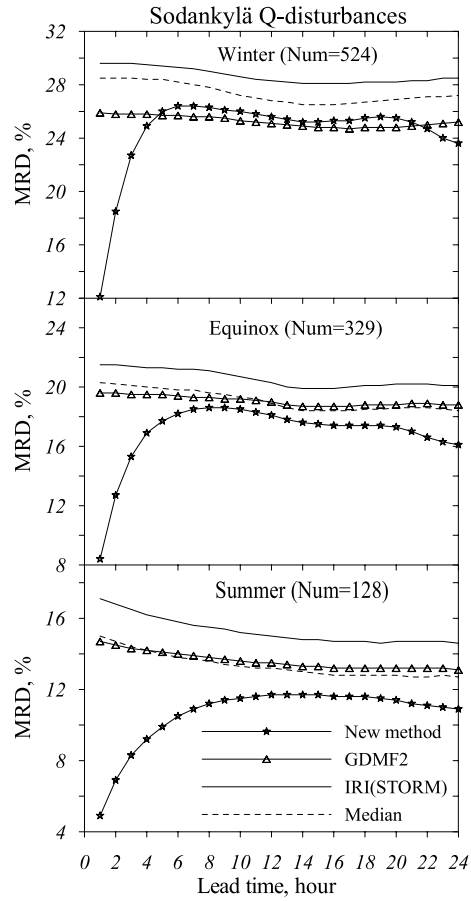

Figure 7. Same as Figure 4 (left column) but for Sodankylä.

On the other hand, a new (1–24) h forecast is done each UT hour when the currently observed foF_2 arrives. Therefore, large forecast mistakes are possible in the initial phase of a magnetic storm. Later, during the main and recovery storm phases, disturbed regression coefficients will be used, which provide an acceptable prediction accuracy (see Table 1).

With respect to F_2-layer negative storm effects starting during daytime hours, one should bear in mind the so-called "forbidden time" for the negative storm onset (Prölss, 1995). Normally, the F_2-layer negative storm phase does not start at middle latitudes during daytime hours. This is due to strong poleward thermospheric wind, which locks disturbed neutral composition to high latitudes. A violation of this rule may take place only under extremely strong magnetic storms like in Figure 8 but they occur very rarely. In practice, this problem may be resolved by using our previous EUROMAP model, which is based on ap indices. If a magnetic forecast is reliable at least 1 day in advance, then the EUROMAP model is able to describe the negative storm phase during daytime hours.

Historical (not less than ~ 30 years) f_oF_2 observations are required to derive a prediction model for a station. Moreover, the station should be "alive" and provide real-time f_oF_2 observations. The number of such stations is limited on a global scale. A relatively long period with observations is necessary to have a sufficient number of really disturbed cases to find regression coefficients. With Q disturbances, the situation is easier and normally about 20–25 years with f_oF_2 observations is sufficient to derive a model.

On the other hand, new ionosondes are being installed all over the world, which provide real-time f_oF_2 observations, while historical data at such stations are absent. The following method may be recommended to use available current observations for global mapping with predicted f_oF_2. Table 1 indicates that the GDMF2 model in general demonstrates better accuracy than IRI (STORM); therefore, it may be used in the future prediction

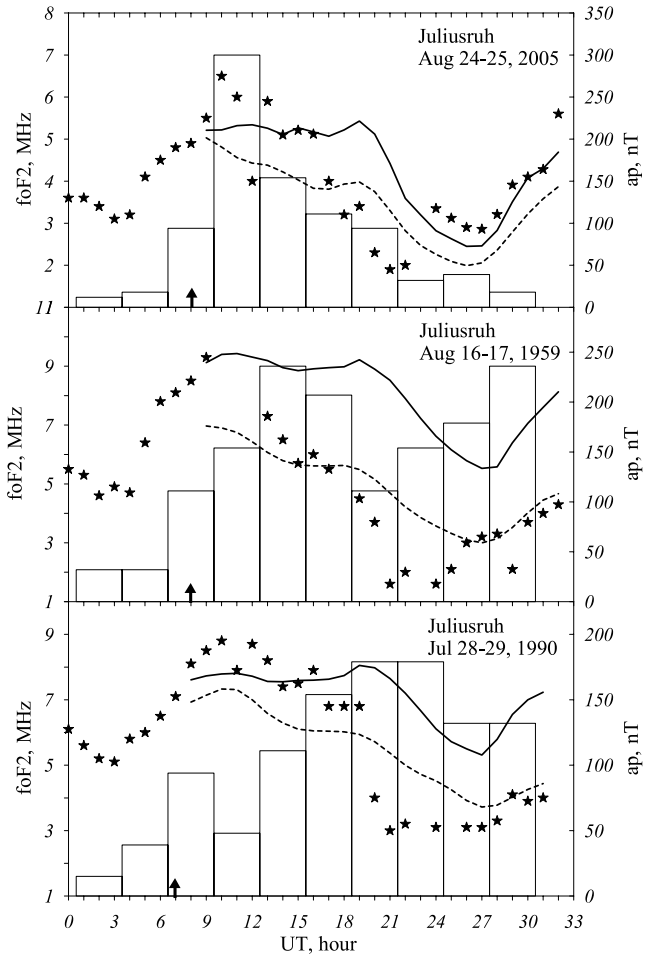

Figure 8. Examples of unsuccessful foF_2 forecasts made at the (UTsr + 4) moment before the onset of severe magnetic storms during daytime hours. Asterisks—foF_2 observations, solid line—Our forecast, dashes—IRI (STORM) predictions, vertical arrows—The moment of forecast, and bars—ap-3h indices (right *y*-axis).

method. The only obvious drawback of this model is the relatively large MRD at small lead times, which is the most important for practice. To overcome this impediment, GDMF2 may be normalized by current f_oF_2 observations to give an f_oF_2 forecast for the next (1–24) hours. Figure 9 gives an example of such GDMF2 normalization at Moscow for quiet and disturbed conditions during three seasons.

Figure 9 shows that the GDMF2 normalization strongly decreases MRD for the first (5–8) lead time hours, while for larger lead times, the original version of GDMF2 may be used. This is quite sufficient for practical applications. Therefore, a possibility to include many additional ionosonde stations for which SRF2 prediction models cannot be created may strongly enlarge the mapping area of predicted f_oF_2.

Along with this, there are "dead" stations with long and good (manually scaled) historical f_oF_2 observations, but real time data are not available from them. Historical observations after their appropriate development can be also used for f_oF_2 short-term predictions. Such a possibility provides our earlier developed EUROMAP model (Kauristie et al., 2021; Mikhailov & Perrone, 2014). This prediction model is driven by ap(τ) indices (Wrenn, 1987), and regression coefficients have been found for disturbed conditions over European stations. Therefore, in principle, local models developed for "dead" stations within the EUROMAP model could be used for the short-term f_oF_2 prediction during disturbed periods.

5. Conclusions

A new method to predict hourly f_oF_2 with a lead time (1–24)h at an ionosonde station has been proposed. About 30 years with hourly f_oF_2 historical observations at a given station are required to derive a local prediction model. Input information to run such a model includes: hourly real-time f_oF_2 observations, a monthly Australian T-index to specify the median f_oF_2 background level, and a predicted level of geomagnetic activity with two gradations: quiet (daily Ap < 30 nT) and disturbed (daily Ap ≥ 30 nT). Testing of the proposed method has shown the following results:

1. The new SRF2 method is able to describe both negative and positive quiet time disturbances occurring under the low (daily Ap < 30 nT) geomagnetic activity. The descriptive accuracy for (1–24) h lead times is significantly (the confidence level >95%) better according to t-criterion than global empirical IRI (STORM) and GDMF2 models provide. This is valid for any season and level of solar activity. Such a result has been obtained for the first time.
2. Similar results are obtained when the SRF2 method manifests at middle latitudes for magnetically disturbed (daily Ap ≥ 30 nT) conditions. The only exception takes place in summer, under large lead times, when GDMF2 provides significantly better results.
3. At the equatorial station, Huancayo, the proposed method manifests the best results both for Q and D conditions but unlike middle latitudes, the running median demonstrates better results for large lead times compared to the global empirical models. The difference between the new method and the running median is significant (at the confidence level >95%) during the first (5–12) h for Q-disturbance cases, while the difference is significant during 4 hr (in summer and winter) and 15 hr at equinox for D-disturbance cases.
4. At Sodankylä station (the auroral zone), due to a lack of observations for magnetically disturbed conditions, a local prediction model could be derived only for Q-disturbances cases. The SRF2 method provides the best results for (1–24) h lead times in summer and equinox, and only for the first 4 hr in winter compared to the GDMF2 model, which systematically manifests better results compared to IRI (STORM).

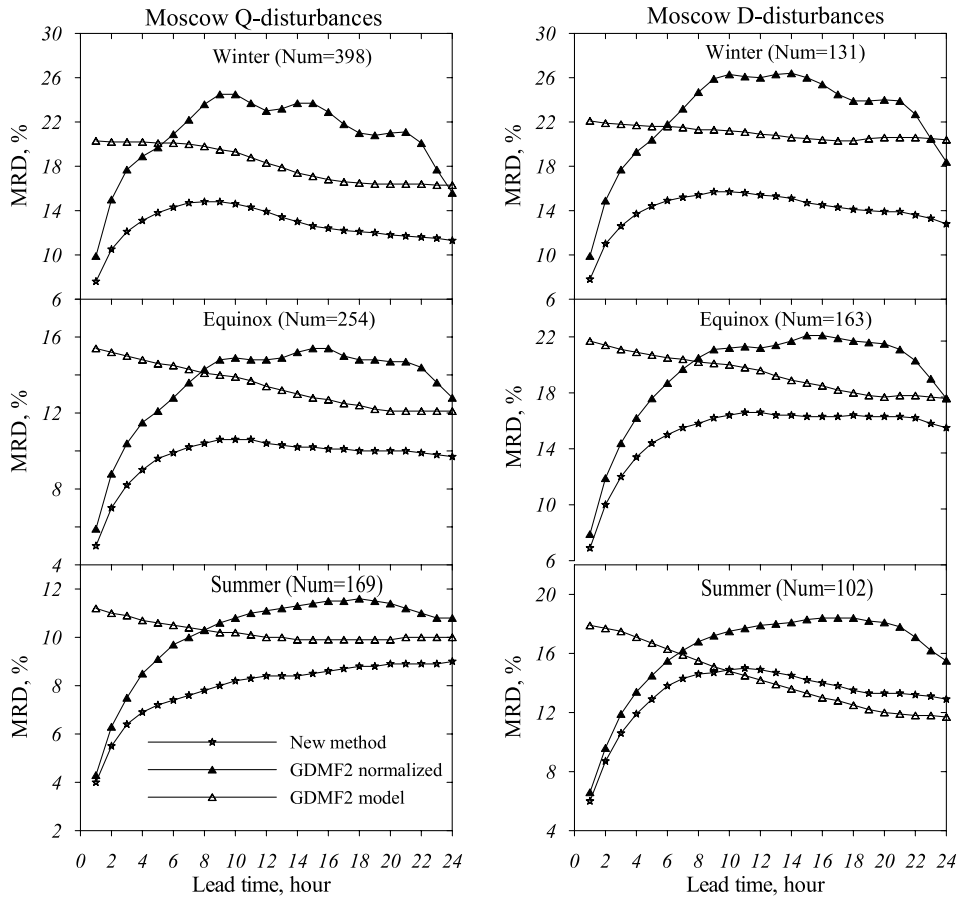

Figure 9. The results of GDMF2 normalization by current f_oF_2 observations that provide the f_oF_2 forecast with (1–24) h lead times. A comparison with the original version of GDMF2 and the newly proposed SRF2 method is given.

5. In general, the proposed SRF2 method may be considered as a practically useful one for f_oF_2 short-term prediction both under magnetically quiet and disturbed conditions. The method as a rule demonstrates significantly better descriptive accuracy compared to modern global empirical models and utilizes all available input information. All these open wide possibilities for its application in practice.

Data Availability Statement

Data is available through the Lowell DIDBase through GIRO for ionosonde data (http://giro.uml.edu/) and for ap geomagnetic index through NOAA SWPC (https://www.swpc.noaa.gov/), GFZ Potsdam (https://www.gfz-potsdam.de/en/kp-index/) and the WDC for Geomagnetism, Kyoto (http://wdc.kugi.kyoto-u.ac.jp/wdc/Sec3.html).

Acknowledgments
This work is supported by INGV-MIUR Project Pianeta Dinamico—The Working Earth (CUP D53J19000170001), Theme 3 SERENA.

References

Araujo-Pradere, E. A., & Fuller-Rowell, T. J. (2002). STORM: An empirical storm-time ionospheric correction model 2. Validation. *Radio Science*, *37*(5), 4–1. https://doi.org/10.1029/2002RS002620

Araujo-Pradere, E. A., Fuller-Rowell, T. J., & Codrescu, M. V. (2002). STORM: An empirical storm-time ionospheric correction model 1. Model description. *Radio Science*, *37*(5), 1–12. https://doi.org/10.1029/2001RS002467

Bruinsma, S., Sutton, E., Solomon, S. C., Fuller-Rowell, T., & Fedrizzi, M. (2018). Space weather modeling capabilities assessment: Neutral density for orbit determination at low Earth orbit. *Space Weather*, *16*(11), 1806–1816. https://doi.org/10.1029/2018SW002027

Caruana, J. (1990). The IPS monthly T index, solar-terrestrial predictions. *Proceedings of a Workshop at Leura*, *2*, 257–263.

Drob, D. P., Emmert, J. T., Meriwether, J. W., Makela, J. J., Doornbos, E., Conde, M., et al. (2015). An update to the Horizontal Wind Model (HWM): The quiet time thermosphere. *Earth and Space Science*, *2*(7), 301–319. https://doi.org/10.1002/2014ea000089

Fejer, B. G., & Scherliess, L. (2001). On the variability of equatorial F-region vertical plasma drifts. *Journal of Atmospheric and Solar-Terrestrial Physics*, *63*(9), 893–897. https://doi.org/10.1016/S1364-6826(00)00198-X

Hedin, A. E. (1987). MSIS-86 thermospheric model. *Journal of Geophysical Research*, *92*(A5), 4649–4662. https://doi.org/10.1029/ja092ia05p04649

Kamide, Y., & Matsushita, S. (1981). Penetration of high-latitude electric fields into low latitudes. *Journal of Atmospheric and Terrestrial Physics*, *43*(5–6), 411–425. https://doi.org/10.1016/0021-9169(81)90105-7

Kauristie, K., Andries, J., Beck, P., Berdermann, J., Berghmans, D., Cesaroni, C., et al. (2021). Space weather services for Civil Aviation—Challenges and solutions. *Remote Sensing*, *13*(18), 3685. https://doi.org/10.3390/rs13183685

Mikhailov, A. V., Depueva, A. K., & Leschinskaya, T. Y. (2004). Morphology of quiet time F_2-layer disturbances: High and lower latitudes. *International Journal of Geomagnetism and Aeronomy*, *5*(1), GI1006. https://doi.org/10.1029/2003GI000058

Mikhailov, A. V., & Mikhailov, V. V. (1999). Indices for monthly median foF2 and M (3000) F2 modelling and long-term prediction. Ionospheric index MF2. *International Journal of Geomagnetism and Aeronomy*, *1*, 141–151.

Mikhailov, A. V., & Perrone, L. (2014). A method for foF2 short-term (1-24) h forecast using both historical and real-time foF2 observations over European stations: EUROMAP model. *Radio Science*, *49*(4), 1–18. https://doi.org/10.1002/2014RS005373

Mikhailov, A. V., Perrone, L., & Nusinov, A. A. (2021). Mid-latitude daytime F2-layer disturbance mechanism under extremely low solar and geomagnetic activity in 2008–2009. *Remote Sensing*, *13*(8), 1514. https://doi.org/10.3390/rs13081514

Mikhailov, A. V., Perrone, L., & Smirnova, N. (2012). Two types of positive disturbances in the daytime mid-latitude F2-layer: Morphology and formation mechanisms. *Journal of Atmospheric and Solar-Terrestrial Physics*, *81–82*, 59–75. https://doi.org/10.1016/j.jastp.2012.04.003

Perrone, L., Mikhailov, A. V., & Nusinov, A. A. (2020). Daytime mid-latitude F_2-layer Q-disturbances: A formation mechanism. *Scientific Reports*, *10*(1), 9997. https://doi.org/10.1038/s41598-020-66134-2

Piggott, W. R., & Rawer, K. U. R. S. I. (1978). *Handbook of ionogram interpretation and reduction; world data center A for solar-terrestrial physics*. National Oceanic and Atmospheric Administration—Environmental Data Service.

Prölss, G. W. (1995). In Volland (Ed.), In *Ionospheric F-region storms, Handbook of Atmospheric Electrodynamics* (Vol. 2, pp. 195–248). CRC Press/Boca Raton.

Rishbeth, H., & Garriott, O. K. (1969). *Introduction to ionospheric physics*. Academic Press.

Rishbeth, H., Jenkins, B., & Moffett, R. J. (1995). The F-layer at sunrise. *Annales Geophysicae*, *13*(4), 367–374. https://doi.org/10.1007/s00585-995-0367-6

Schunk, R. W., Gardner, L., Scherliess, L., & Zhu, L. (2012). Problems associated with uncertain parameters and missing physics for long-term ionosphere-thermosphere forecasting. *Radio Science*, *47*(4), RS0L23. https://doi.org/10.1029/2011RS004911

Shim, J. S., Kuznetsova, M., Rastatter, L., Bilitza, D., Butala, M., Codrescu, M., et al. (2012). CEDAR Electrodynamics Thermosphere Ionosphere (ETI) Challenge for systematic assessment of ionosphere/hermosphere models: Electron density, neutral density, NmF2, and hmF2 using space based observations. *Space Weather*, *10*, S10004. https://doi.org/10.1029/2012SW000851

Shim, J. S., Kuznetsova, M., Rastatter, L., Hesse, M., Bilitza, D., Butala, M., et al. (2011). CEDAR electrodynamics thermosphere ionosphere (ETI) challenge for systematic assessment of ionosphere/hermosphere models: NmF2, and hmF2, and vertical drift using ground-based observations. *Space Weather*, *9*(12), S12003. https://doi.org/10.1029/2011SW000727

Shubin, V. N., & Deminov, M. G. (2019). Global Dynamic model of critical frequency of the ionospheric F2 layer. *Geomagnetism and Aeronomy*, *59*(4), 429–440. https://doi.org/10.1134/s0016793219040157

Tsagouri, I., Goncharenko, L., Shim, J. S., Belehaki, A., Buresova, D., & Kuznetsova, M. M. (2018). Assessment of current capabilities in modeling the ionospheric climatology for space weather applications: FoF2 and hmF2. *Space Weather*, *16*(12), 1930–1945. https://doi.org/10.1029/2018sw002035

Turner, J. F. (1968). The development of the ionospheric index T, IPS Series R, Report (Vol. *R11*).

Wrenn, G. L. (1987). Time-weighted accumulations ap(τ) and Kp(τ). *Journal of Geophysical Research*, *92*(A9), 10125–10129. https://doi.org/10.1029/ja092ia09p10125

Wrenn, G. L., Rodger, A. S., & Rishbeth, H. (1987). Geomagnetic storms in the Antarctic F-region. I. Diurnal and seasonal patterns for main phase effects. *Journal of Atmospheric and Terrestrial Physics*, *49*(9), 901–913. https://doi.org/10.1016/0021-9169(87)90004-3